Perovskite solar cells with embedded homojunction via nonuniform metal ion doping

Lin, Yuze; Li, Tao; Liu, Ye; Bahrami, Behzad; Guo, Dengyang; Fang, Yanjun; Shao, Yuchuan; Wang, Qi; Savenije, Tom J.; More Authors

DOI
10.1016/j.xcrp.2021.100415

Publication date
2021

Document Version
Final published version

Published in
Cell Reports Physical Science

Cell Reports
Physical Science

CellPress
OPEN ACCESS

Article

Perovskite solar cells with embedded homojunction via nonuniform metal ion doping

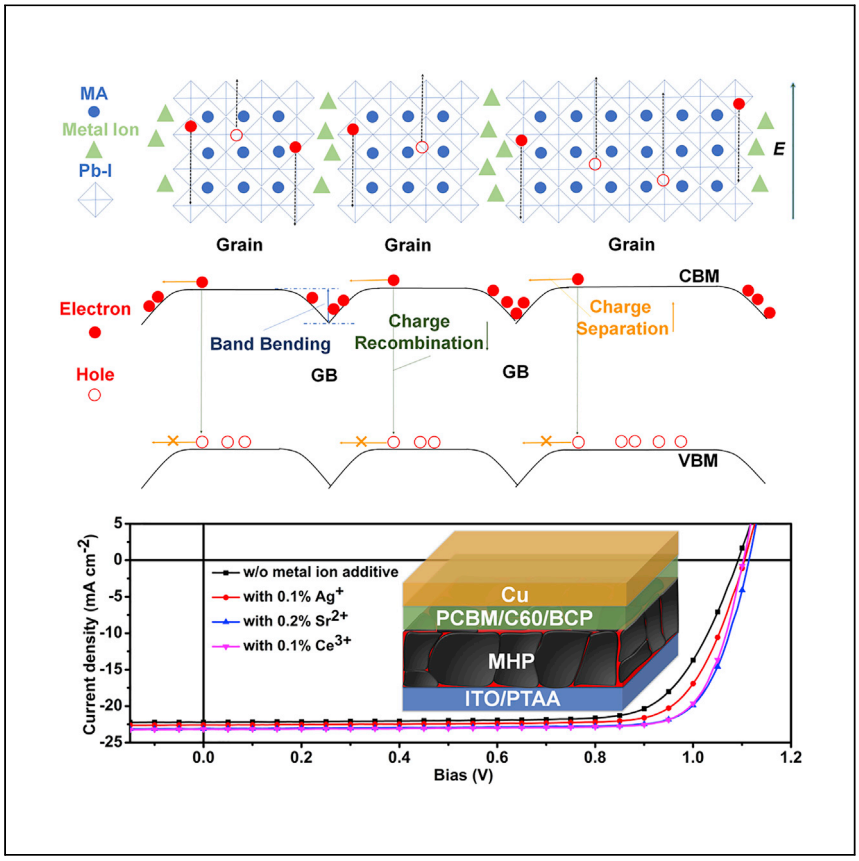

Lin et al. report the nonuniform doping of perovskite polycrystalline films by several metal ions and the homojunctions formed within each individual grain. The built-in electric field within each grain reduces the recombination of charge carriers at grain boundaries and grain interiors, leading to increased efficiency of perovskite solar cells.

Yuze Lin, Tao Li, Ye Liu, ..., Tom J. Savenije, Qiquan Qiao, Jinsong Huang

jhuang@unc.edu

Highlights

Nonuniform metal ion doping for perovskite polycrystalline thin films

Lateral homojunction formed within each individual perovskite grain

Charge recombination reduced by built-in electric field within each grain

Lin et al., Cell Reports Physical Science 2, 100415
May 19, 2021
https://doi.org/10.1016/j.xcrp.2021.100415

Cell Reports
Physical Science

CellPress
OPEN ACCESS

Article

Perovskite solar cells with embedded homojunction via nonuniform metal ion doping

Yuze Lin,[1] Tao Li,[2] Ye Liu,[1] Behzad Bahrami,[5] Dengyang Guo,[4] Yanjun Fang,[6] Yuchuan Shao,[1] Ashraful Haider Chowdhury,[5] Qi Wang,[1] Yehao Deng,[1] Alexei Gruverman,[2] Tom J. Savenije,[4] Qiquan Qiao,[3] and Jinsong Huang[1,6,7,*]

SUMMARY

A long photoluminescence decay lifetime has been regarded as a generic indication of long charge carrier recombination lifetime in semiconductors such as metal halide perovskites (MHPs), which have shown tremendous success in solar cells. Here, we report that MHP polycrystalline films with extrinsic metal ions have a very long charge recombination lifetime, but a much shorter photoluminescence decay lifetime, and this huge difference can be explained by a model of lateral homojunction within each individual grain. The lateral homojunction is formed due to the doping along grain boundaries by metal ions, and then verified by nanoscale potential mapping and transient photo-response mapping. The built-in electric field within each grain reduces the recombination of free charge carriers within the perovskite grain and along grain boundaries, while the free electrons and holes are collected to cathode and anode through the grain boundaries and grain interiors, respectively. Then, the efficiencies of MHP polycrystalline solar cells are increased.

INTRODUCTION

The history of efficiency enhancement for thin-film solar cells has witnessed the importance of reducing charge-recombination loss within devices, including both at the electrode contacts and inside the photoactive layers.[1-5] A long charge carrier recombination lifetime in semiconductor materials, including metal halide perovskites (MHPs) have shown tremendous success in solar cell applications.[6-16] Many efforts have been devoted to increase the carrier recombination lifetime in polycrystalline MHP solar cells by increasing the grain size and crystallinity via film growth modification[16-18] and by passivating charge traps either on the surface or at grain boundaries (GBs) of perovskite films.[19-24] Photoluminescence (PL) intensity and decay lifetime are generally used to characterize the charge recombination lifetime due to its simplicity to measure.

Extrinsic metal ions have been investigated in MHPs on their influence of PL intensity, lifetime, and the device performance.[25] Several metal ions, such as K^+, Na^+, Rb^+, Ca^{2+}, Cd^{2+}, Al^{3+}, and Eu^{3+}, have been added into MHP thin films as additives to increase the PL intensity and/or lifetimes and then improve the device efficiency of MHP solar cells. K^+, Na^+, and Cd^{2+} ions have shown defect passivation effect in perovskite thin films[26-28]; Na^+ was also reported to reduce disorder and nonradiative recombination rate within perovskite thin films; Rb^+ was initially thought to form an alloy with perovskites, but was later found to mainly stay at GBs and play a similar

[1]Department of Applied Physical Sciences, University of North Carolina, Chapel Hill, NC 27599, USA

[2]Department of Physics and Astronomy, University of Nebraska-Lincoln, Lincoln, NE 68588, USA

[3]Department of Mechanical and Aerospace Engineering, Syracuse University, Syracuse, NY 13244, USA

[4]Opto-electronic Materials Section, Department of Chemical Engineering, Delft University of Technology, van der Maasweg 9, 2629 HZ Delft, the Netherlands

[5]Department of Electrical Engineering, Center for Advanced Photovoltaics, South Dakota State University, Brookings, SD 57007, USA

[6]Department of Mechanical and Materials Engineering, University of Nebraska-Lincoln, Lincoln, NE 68588, USA

[7]Lead contact

*Correspondence: jhuang@unc.edu

https://doi.org/10.1016/j.xcrp.2021.100415

role with K^+.[29] The addition of Ca^{2+} could improve perovskite crystallinity and thus reduce defect density[30]; Al^{3+} was also reported to improve the quality of thin films with reduced nonuniform strain[31]; Eu^{3+} was used to reduce the formation of Pb^0 and I^0 under illumination and improve the photostability of MHPs due to the redox shuttle of Eu^{3+}/Eu^{2+}.[32] Recently, we demonstrated that Ag^+, Sr^{2+}, and Ce^{3+} ions could heavily dope the surface of perovskites even into metallic in some cases, and they preferred to stay at perovskite surfaces, leaving the interior of perovskite grains much less doped.[33] This nonuniform doping of metal ions provides a chance to form homojunctions in polycrystalline perovskite thin films between individual perovskite grains and their adjacent GBs and/or surface.

In this work, we show that MHP polycrystalline films with extrinsic metal ions dopants have a very long charge recombination approaching 5 μs measured by time-resolved microwave conductance (TRMC), but a much shorter PL decay lifetime of tens of nanoseconds, which is different from the reported passivated ions mentioned above. A model of lateral p-n homojunction within each individual grain is proposed to explain the huge difference in measured charge recombination lifetimes. The lateral p-n junction is formed due to the doping along GBs by metal ions; then the built-in electric field within each grain reduces the recombination of free electrons and holes, while the free electrons and holes are collected to cathode and anode through the GBs and grain interiors, respectively. The reduced charge recombination results in the increased efficiency of MHP polycrystalline solar cells.

RESULTS

PL decay and charge carrier recombination lifetime

Several types of metal ions, including Ag^+, Sr^{2+}, and Ce^{3+} ions, which have been demonstrated to dope the perovskite surface,[33] were added into polycrystalline MHP films to study the influence on the performance of MHP solar cells. In contrast to some other ions such as Na^+, K^+, and Rb^+, which generally passivate perovskite defect, these ions were found to behave like n-type dopants and that the highest occupied level of Ag, Sr, and Ce are closer to the conduction band minimum (CBM) of the methylammonium iodide (MAI)- or PbI_2-terminated surface.[33] Here, we found that the addition of 0.1%–0.2% (weight ratio) of metal ions with different valence charges, including Ag^+, Sr^{2+}, and Ce^{3+}, into methylammonium lead iodide ($MAPbI_3$) thin films can quench their PL by 40%–87% (Figure S1). It should be noted here that all of the impurity elements of high-purity commercial PbI_2 are at the level of parts per million (ppm)—for example, Ag < 0.1 ppm, Sr < 0.05 ppm, and Ce < 0.05 ppm, which are much lower than what we added in the perovskite precursor solution. The PL quenching effect is confirmed by the study of PL lifetime variation using time-resolved PL (TRPL) measurement. As shown by the PL decay curves in Figure 1A, the pristine $MAPbI_3$ film deposited on glass shows PL decay lifetimes with a maximum value of ~2.0 μs, but the addition of all types of metal ions (Ag^+, Sr^{2+}, and Ce^{3+}) dramatically reduces PL decay lifetime down to 40–130 ns. Even in the stacking structures with both electron and hole transport layers, these metal ion additives further decrease the TRPL lifetime of $MAPbI_3$ (Figure S2). $MAPbI_3$ films with metal ion additives made by other deposition methods such as blade coating showed the same PL quenching behavior (Figure S3). Surprisingly, these metal ion additives increased the power conversion efficiencies (PCEs) of MHP solar cells, once the amount of the added ions was optimized. We evaluated the impact of ion addition to device performance in solar cell devices with a p-i-n structure of indium tin oxide (ITO)/poly[bis(4-phenyl)(2,4,6-trimethylphenyl)amine] (PTAA)/MHP/[6]-phenyl-C61-butyric acid methyl ester (PCBM)/C_{60}/bathocuproine (BCP)/copper (Cu), as shown

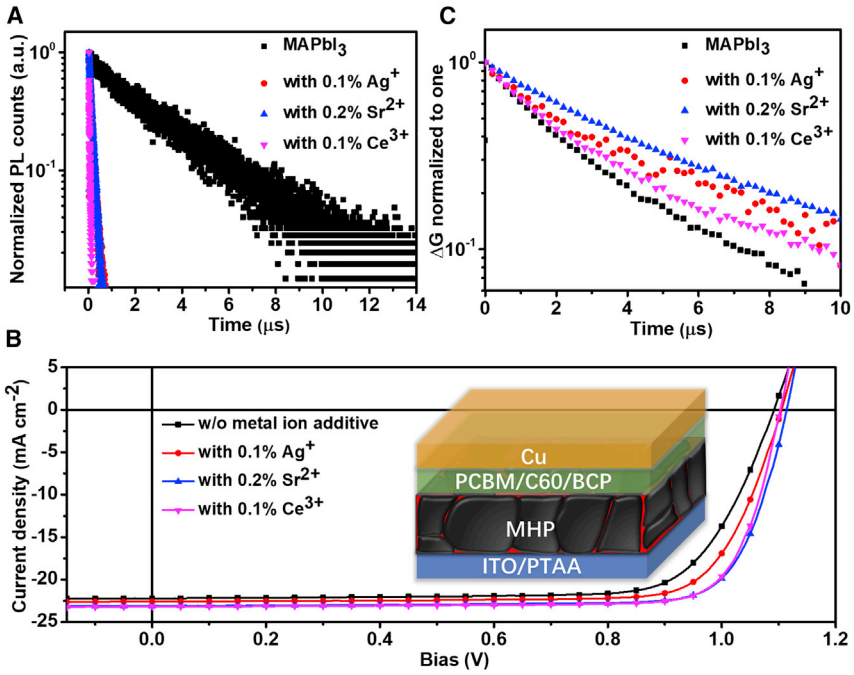

Figure 1. Lifetime measurement and device performance

(A) TRPL decay curves of $MAPbI_3$ with or without metal ion additives.

(B) J-V curves of $FA_{0.85}MA_{0.15}Pb(I_{0.85}Br_{0.15})$-based solar cells blending with metal ions. The inset is the device structure of perovskite solar cells: ITO/PTAA/MHP/PCBM/C60/BCP/Cu.

(C) TRMC traces of $MAPbI_3$ with or without metal ion additives.

in Figure 1B. The MHP layers have the compositions of $MAPbI_3$ or $FA_{0.85}MA_{0.15}Pb(I_{0.85}Br_{0.15})_3$, where FA is formamidinium. The PCEs of the $MAPbI_3$ devices with the addition of these extrinsic metal ions (Ag^+, Sr^{2+}, Ce^{3+}) were improved from 17.4% to 18.6%–19.4% after these ion contents were optimized, which varied from 0.07% to 0.2% (Table S1). Similarly, the addition of these extrinsic metal ions increased the stabilized PCEs of $FA_{0.85}MA_{0.15}Pb(I_{0.85}Br_{0.15})_3$ solar cells from 18.7% to 20.8% (Figure 1B; Table S1), and the photocurrent curves showed negligible current hysteresis (Figure S4). Relative to the control device based on $FA_{0.85}MA_{0.15}Pb(I_{0.85}Br_{0.15})_3$ without any additive, the device with Ce^{3+} doping showed higher external quantum efficiency in whole spectra, with 1.9 mA cm^{-2} higher integrated current density (Figure S5). From the PCE statistics of 30 solar cells with and without metal ions, >60% of the solar cells with Sr^{2+} or Ce^{3+} showed PCEs higher than 19% (Figure S4), which is better than those of the control devices without dopants. The very small amount (0.1%–0.2%) of extrinsic metal ion additives do not obviously affect the light stability of the devices, while a high concentration (5%) of Sr^{2+} or Ce^{3+} increases the light stability of the $MAPbI_3$ films (Figure S6).

Although the solar cell efficiencies have not reached the record values, it is very interesting that the addition of a very small amount of extrinsic ions reduced the PL, while it enhanced the device efficiency and device yield. To understand this unusual behavior, we measured free carrier recombination lifetimes by TRMC in the MHP films doped by extrinsic metal ions. The excitation light has a wavelength of 500 nm and large fluence of 7 ± 4 nJ cm^{-2}, which is close to that in the TRPL measurement. It generates a charge carrier concentration of $(3.6 \pm 2.1) \times 10^{14}$ cm^{-3}, which is large enough to avoid artifacts in the photoconductivity measurement

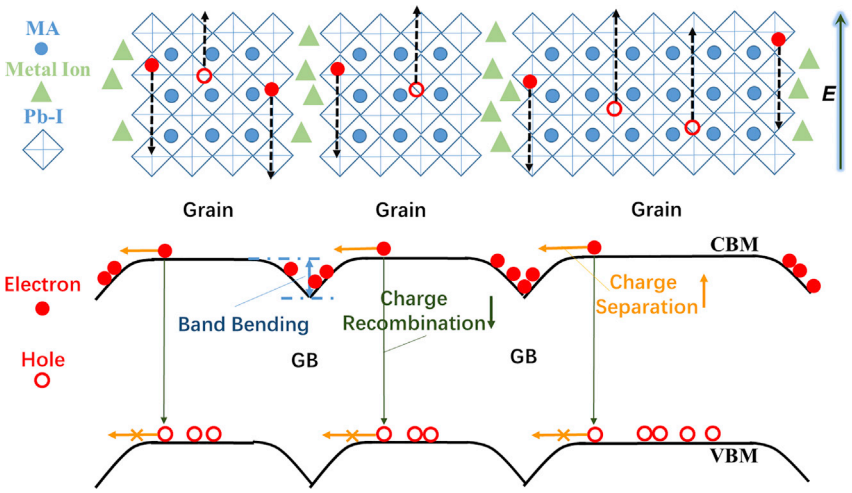

Figure 2. Proposed model of lateral homojunction

The proposed scheme of the model of metal ion doping MHP. Using $MAPbI_3$ as an example, where the metal ions gathered in GBs of MHP thin film, and then downshifted band bending toward GBs; the charge separation increases and recombination decreases.

caused by minority carrier traps or depletion-region modulation[34,35]; the detailed analysis can be found in the supplemental experimental procedures and Figures S7–S10. We selected univalent Ag^+, divalent Sr^{2+}, and trivalent Ce^{3+} to be blended with $MAPbI_3$ deposited on quartz for this study. The excitation laser with a 500-nm wavelength, which was used in TRMC measurement, cannot excite the metal halide we added here, such as AgI with 440 nm absorption onset, to generate photocarriers, which can exclude the potential effect of the long-lifetime photocarriers in AgI itself on the TRMC lifetime assessment of perovskite thin films. As shown in Figure 1C, the free carrier decay lifetime in pristine $MAPbI_3$ measured by TRMC is 2.1 μs, comparable to the measured PL decay lifetime of up to 2.0 μs, indicating a weak surface charge recombination due to the high quality of these films formed by our established methods.[19] In striking contrast, the samples with metal ion additives display very long free carrier decay lifetimes of 4.1, 4.9, and 3.0 μs for the $MAPbI_3$ films blended with 0.1 wt% Ag^+, 0.2 wt% Sr^{2+}, and 0.1 wt% Ce^{3+}, respectively. These longer free carrier recombination lifetimes coincided with the better device performance of MHP solar cells with metal ion additives. Fitting of the TRMC traces under varied excitation light intensity using a simple model[33] shows minority charge trapping density reduced upon metal ion doping (Figure S7).

Lateral homojunction model

We propose a model illustrated in Figure 2 to explain the enhanced efficiency in perovskite solar cells with the addition of extrinsic metal ions and the discrepancy between the long TRMC carrier lifetimes and the very short PL lifetimes. Since the metal ions stay in the polycrystalline perovskite films after deposition and our previous study has revealed negligible incorporation of these ions into perovskite crystal structures, they should accumulate in GBs and/or the surface of MHPs and cause n-doping there. A nearly intrinsic grain interior and a doped GB form a homojunction inside each individual perovskite grain. A doping-induced built-in electric field in each grain separates the photogenerated electron-hole pairs, which quenches PL and reduces the PL lifetime, while the spatial separation of free electrons and holes slows down their recombination and increases the free carrier recombination lifetime of MHP thin film and solar cells. The introduced halide counterions may also affect

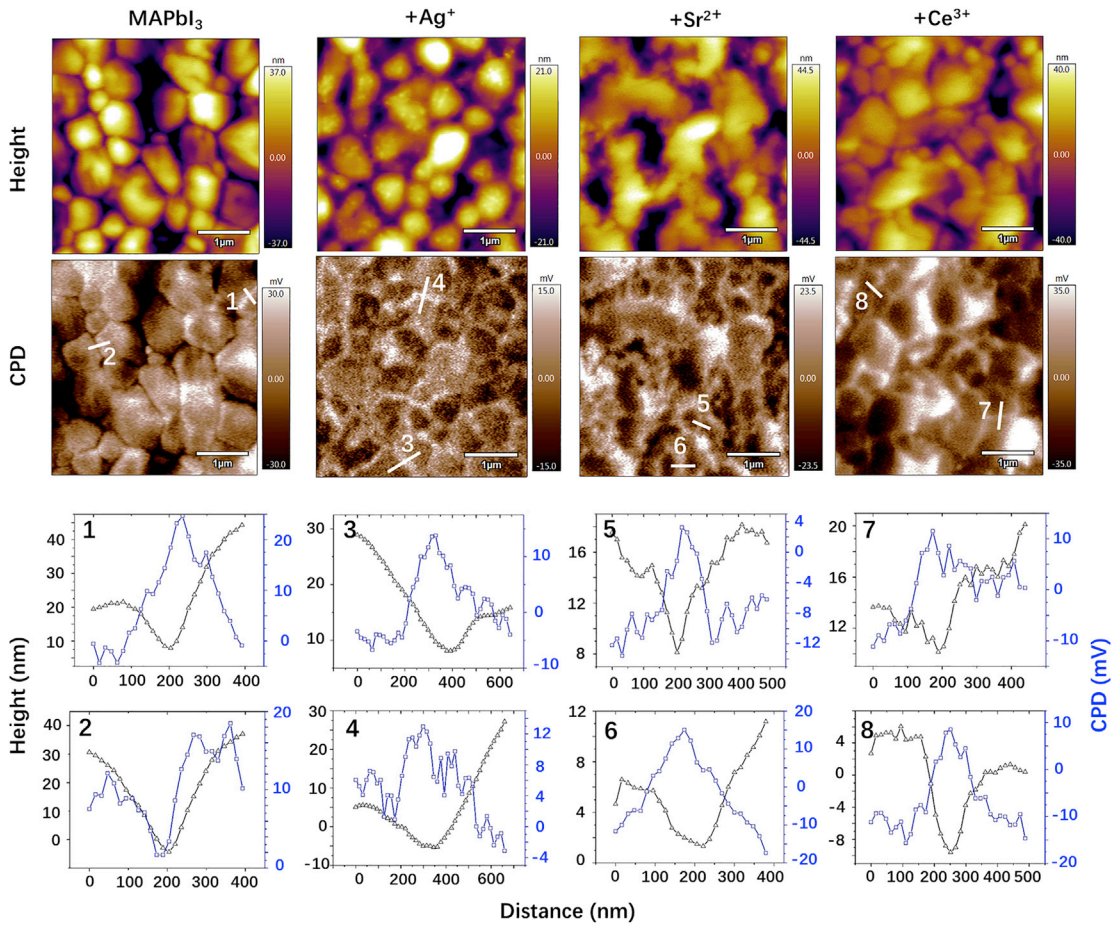

Figure 3. Potential distribution

Height and CPD images of $MAPbI_3$ thin films blending without and with 0.1% Ag^+, 0.2% Sr^{2+}, and 0.1% Ce^{3+}, respectively. Eight grain boundaries are labeled in the CPD images, and their height and CPD across the grain boundaries are displayed.

the doping efficiency, if they can change the surface or GB defect density, which is to be determined by future study. The filling of some I^- vacancies may compensate partially the n-doping from the extrinsic metal ions. However, electric measurements showed that the perovskite surface with metal halide additives is largely n-doped, indicating the doping effect is dominated by the introduced extrinsic metal ions.

Nanoscale potential mapping

To verify the formation of the homojunction at grain level, we conducted Kelvin probe force microscopy (KPFM) measurement to find out the potential distribution of perovskite polycrystalline films at the grain scale. Here, we mechanically polished MHP thin films to avoid the impact of the surface composition heterogeneity on surface work function distribution and possible surface doping by the metal ions.[36] Figure 3 shows the KPFM potential images of $MAPbI_3$ thin films without and with Ag^+, Sr^{2+}, and Ce^{3+} ions, respectively. The contact potential difference (CPD) in the measurements is defined as $(\Phi_{tip} - \Phi_{sample})/e$. We used the same type of conductive tip (i.e., consistent Φ_{tip}); thus, the CPD value should be directly related to the work function of the measured samples. Compared to the grain interiors, both upward and downward band bending at the GBs are observed in the same pristine $MAPbI_3$ thin films, evidenced by the brighter and darker colors, respectively. From the CPD image in

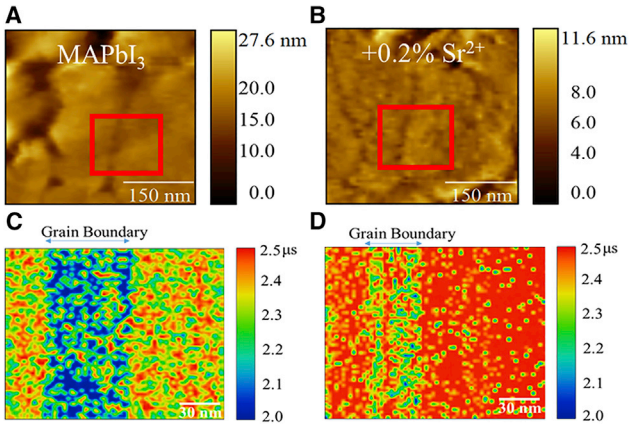

Figure 4. Charge carrier dynamics mapping

Contact mode AFM topography (A and B) of polished $MAPbI_3$ perovskite films without (A and C) and with 0.2% Sr^{2+} (B and D) and their corresponding TP-AFM-resolved mapping of charge carrier lifetime (C and D).

Figure 3, one can find that ~80% of the GBs in the pristine $MAPbI_3$ films were still darker (or higher work function) than the grain interior, while the other fraction GBs were brighter (or lower work function) than the grain interior. The CPD difference between GBs and their adjacent grains in the pristine $MAPbI_3$ thin film was between ~−25 and 50 mV, which can be explained by the composition variation-induced self-doping of perovskites.[37-40] Our previous study showed that MAI-rich $MAPbI_3$ displays p-type behavior, while PbI_2-rich perovskite displays n-type behavior.[41] Thermal annealing may cause the evaporation of MAI, turning some GBs into the n-type, while the grain interior may remain weakly p-type. There is a variation of heterogeneity among different films prepared under different thermal annealing conditions. In contrast, almost all $MAPbI_3$ films blended with Ag^+, Sr^{2+}, and Ce^{3+} ions show n-type GBs with energy levels bending toward the Fermi level (i.e., brighter than the grain interior, which means the reduced work function in GBs than those in grains). In $MAPbI_3$ films blended with all types of metal ions, the CPD at GBs were larger than those of their grain interiors, as shown by the cross-sectional CPD curves in Figure 3 and the statistics of ΔCPD between grains and their adjacent GBs in Figure S11. Thus, the extrinsic metal ions accumulating at GBs lead to Fermi-level pinning of perovskite at the GBs, which causes the observed band bending and n-type doping behavior in the peripheral area of perovskite grains. It should be noted that the CPD difference between the grain interior and GBs measured here is expected to be smaller than the actual value, because of the limited lateral resolution of the KPFM (tens of nanometers). This result confirmed the n-type doping of the perovskite along the GBs and the formation of lateral homojunctions at the grain level between the grain center and GBs by extrinsic metal ion doping.

Charge carrier dynamics mapping

Charge carrier dynamics at the grain interior and GBs of perovskite thin films with and without metal ion doping were mapped at the nanoscale using the recently developed transient photo-response atomic force microscopy (TP-AFM).[42,43] A TP-AFM tip was placed and scanned on the surface of the perovskite film to collect the light-induced charge carriers for measuring nanoscale charge carrier dynamics such as apparent carrier recombination lifetime. Here, MHP thin films were also mechanically polished to avoid the impact from the surface. Figures 4A and 4B show 400 × 400 nm contact mode AFM topography images of polished $MAPbI_3$

perovskite films without and with 0.2% Sr^{2+} perovskite films, respectively. The 150 × 150 nm area that includes the GBs on the topography image (indicated by the red square) was selected for the nanoscale charge dynamics mapping. A longer carrier recombination lifetime would indicate improved local charge carrier dynamics. The apparent carrier recombination lifetime was imaged to reveal spatial variations at GBs of perovskite films before and after metal ion doping. As shown in Figure 4, Sr^{2+} doped $MAPbI_3$ thin films showed improved charge carrier recombination lifetimes at both grain interiors and GBs, compared to the $MAPbI_3$ film without additive, which is consistent with the lateral homojunction model we propose above. The mean of apparent charge carrier lifetimes at GB in the 0.2% Sr^{2+} perovskite films (~2.40 μs) sample is longer than that of the control sample (~2.12 μs).

Electroluminescence (EL)

One question arises as to why the MHP solar cells with these metal ions still have comparable open circuit voltage (V_{OC}) with the pristine ones, since the PL quantum yield (PLQY) is significantly lower. It is noted that the PLQYs of semiconductor films are broadly used to evaluate the quality of nonbulk heterojunction-type thin film photovoltaic materials, and it is often observed that a large PLQY of perovskite films results in a larger device V_{OC}. We argue that one should analyze the device V_{OC} deficit using external EL efficiency of a solar cell under forward bias, since it represents the reciprocal operation condition of a solar cell under illumination, which is in agreement with recent practice.[5] The external quantum efficiency (EQE) of a light-emitting diode (LED) is not only determined by the radiative charge recombination but is also related to charge transport, which is more relevant to the operation of a real solar cell device. This also explains why some quantum dots (QDs) with almost unity PLQY cannot be directly transferred to a high V_{OC} in solar cells, because the ligands of QDs impede the charge injection to QDs. In our case, the formed doped channels help not only the charge extraction in solar cells but also the injection of electrons and holes into perovskites when the device operates as a LED. The measured maximum electroluminescence EQE (EQE_{EL}) of solar cells based on $MAPbI_3$ with metal ions additives increased from 0.02% to 0.032%–0.04% (Figure S12), compared with the control device without additives, indicating that the metal ion additives do not put a higher ceiling for the V_{OC} of perovskite solar cells. This agrees with the TRMC measurement results that no more nonradiative charge recombination channels were introduced by ion doping. Actually, the reduced trap density from the TRMC measurement indicates that the LED may even have a larger efficiency. The longer charge carrier recombination lifetimes in perovskite active layers, along with higher device EQE_{EL}, coincided with the better device photovoltage and performance of MHP solar cells with metal ion additives.

DISCUSSION

In summary, we found that the addition of the metal ions quenched radiative charge recombination while they dramatically slow down the bimolecular charge recombination in MHPs. Then, a model of lateral homojunction was proposed in MHP thin films blended with extrinsic metal ions. The presence of a homojunction in individual perovskite grains in doped films should have a strong impact on the light to current conversion process in solar cells in many ways, such as minimizing the charge recombination by separating photogenerated electrons and holes spatially into different transport channels and facilitating the charge separation in low-dimensional perovskites. The electron-hole separation also makes the materials less sensitive to

defects at GBs. The homojunction formed by the doping concept can be broadly applied to other MHP applications in which a long carrier recombination lifetime is needed, such as photodetectors and radiation detectors.

EXPERIMENTAL PROCEDURES

Resource availability

Lead contact

Further information and requests for resources and materials should be directed to and will be fulfilled by the lead contact, Jinsong Huang (jhuang@unc.edu).

Materials availability

This study did not generate new unique materials.

Data and code availability

The published article includes all of the data analyzed and necessary to draw the conclusions of this study in the figures and tables of the main text and supplemental information. Further information and requests for additional data should be directed to the lead contact.

SUPPLEMENTAL INFORMATION

Supplemental information can be found online at https://doi.org/10.1016/j.xcrp.2021.100415.

ACKNOWLEDGMENTS

The work is financially supported by the Center for Hybrid Organic Inorganic Semiconductors for Energy (CHOISE), an Energy Frontier Research Center funded by the Office of Basic Energy Sciences, Office of Science within the US Department of Energy, and the National Science Foundation through the Nebraska Materials Research Science and Engineering Center (MRSEC) (grant no. DMR-1420645).

AUTHOR CONTRIBUTIONS

J.H. conceived the idea. J.H. and Y. Lin designed the experiments. Y. Lin fabricated and characterized the solar cells. T.L. and A.G. conducted the KPFM characterization. Y. Liu contributed to fabricating and polishing the thin film samples. B.B., A.H.C., and Q.Q. conducted the TP-AFM characterization. D.G. and T.J.S. conducted the TRMC characterization. Y.F., Y. Liu, and Y.S. conducted the PL and TRPL characterizations. Q.W. contributed to the EQE_{EL} measurement. Y.D. fabricated the blade-coated thin films. J.H. and Y. Lin wrote the paper. All of the authors reviewed the paper.

DECLARATION OF INTERESTS

J.H. is a board member of *Cell Reports Physical Science*. J.H. and Y. Lin are inventors on a patent application related to this work filed by the University of North Carolina, Chapel Hill. The other authors declare no competing interests.

Received: January 27, 2021
Revised: March 15, 2021
Accepted: April 6, 2021
Published: April 26, 2021

REFERENCES

1. Ni, Z., Bao, C., Liu, Y., Jiang, Q., Wu, W.Q., Chen, S., Dai, X., Chen, B., Hartweg, B., Yu, Z., et al. (2020). Resolving spatial and energetic distributions of trap states in metal halide perovskite solar cells. Science *367*, 1352–1358.
2. Son, D.Y., Lee, J.W., Choi, Y.J., Jang, I.H., Lee, S., Yoo, P.J., Shin, H., Ahn, N., Choi, M., and Kim, D. (2016). Self-formed grain boundary healing layer for highly efficient $CH_3NH_3PbI_3$ perovskite solar cells. Nat. Energy *1*, 16081.
3. Tang, J., Kemp, K.W., Hoogland, S., Jeong, K.S., Liu, H., Levina, L., Furukawa, M., Wang, X., Debnath, R., Cha, D., et al. (2011). Colloidal-quantum-dot photovoltaics using atomic-ligand passivation. Nat. Mater. *10*, 765–771.
4. Oh, J., Yuan, H.C., and Branz, H.M. (2012). An 18.2%-efficient black-silicon solar cell achieved through control of carrier recombination in nanostructures. Nat. Nanotechnol. *7*, 743–748.
5. Bi, D., Tress, W., Dar, M.I., Gao, P., Luo, J., Renevier, C., Schenk, K., Abate, A., Giordano, F., Correa Baena, J.P., et al. (2016). Efficient luminescent solar cells based on tailored mixed-cation perovskites. Sci. Adv. *2*, e1501170.
6. Kojima, A., Teshima, K., Shirai, Y., and Miyasaka, T. (2009). Organometal halide perovskites as visible-light sensitizers for photovoltaic cells. J. Am. Chem. Soc. *131*, 6050–6051.
7. Dong, Q., Fang, Y., Shao, Y., Mulligan, P., Qiu, J., Cao, L., and Huang, J. (2015). Solar cells. Electron-hole diffusion lengths > 175 μm in solution-grown CH3NH3PbI3 single crystals. Science *347*, 967–970.
8. Shi, D., Adinolfi, V., Comin, R., Yuan, M., Alarousu, E., Buin, A., Chen, Y., Hoogland, S., Rothenberger, A., Katsiev, K., et al. (2015). Solar cells. Low trap-state density and long carrier diffusion in organolead trihalide perovskite single crystals. Science *347*, 519–522.
9. deQuilettes, D.W., Vorpahl, S.M., Stranks, S.D., Nagaoka, H., Eperon, G.E., Ziffer, M.E., Snaith, H.J., and Ginger, D.S. (2015). Solar cells. Impact of microstructure on local carrier lifetime in perovskite solar cells. Science *348*, 683–686.
10. Huang, J., Yuan, Y., Shao, Y., and Yan, Y. (2017). Understanding the physical properties of hybrid perovskites for photovoltaic applications. Nat. Rev. Mater. *2*, 17042.
11. Snaith, H.J. (2013). Perovskites: The Emergence of a New Era for Low-Cost, High-Efficiency Solar Cells. J. Phys. Chem. Lett. *4*, 3623–3630.
12. Yang, W.S., Park, B.W., Jung, E.H., Jeon, N.J., Kim, Y.C., Lee, D.U., Shin, S.S., Seo, J., Kim, E.K., Noh, J.H., and Seok, S.I. (2017). Iodide management in formamidinium-lead-halide-based perovskite layers for efficient solar cells. Science *356*, 1376–1379.
13. Li, X., Bi, D., Yi, C., Décoppet, J.-D., Luo, J., Zakeeruddin, S.M., Hagfeldt, A., and Grätzel, M. (2016). A vacuum flash-assisted solution process for high-efficiency large-area perovskite solar cells. Science *353*, 58–62.
14. Deng, Y., Ni, Z., Palmstrom, A.F., Zhao, J., Xu, S., Van Brackle, C.H., Xiao, X., Zhu, K., and Huang, J. (2020). Reduced Self-Doping of Perovskites Induced by Short Annealing for Efficient Solar Modules. Joule *4*, 1949–1960.
15. Xiao, M., Huang, F., Huang, W., Dkhissi, Y., Zhu, Y., Etheridge, J., Gray-Weale, A., Bach, U., Cheng, Y.B., and Spiccia, L. (2014). A fast deposition-crystallization procedure for highly efficient lead iodide perovskite thin-film solar cells. Angew. Chem. Int. Ed. Engl. *53*, 9898–9903.
16. Hu, H., Qin, M., Fong, P.W.K., Ren, Z., Wan, X., Singh, M., Su, C.J., Jeng, U.S., Li, L., Zhu, J., et al. (2021). Perovskite Quantum Wells Formation Mechanism for Stable Efficient Perovskite Photovoltaics-A Real-Time Phase-Transition Study. Adv. Mater. *33*, e2006238.
17. Bi, C., Wang, Q., Shao, Y., Yuan, Y., Xiao, Z., and Huang, J. (2015). Non-wetting surface-driven high-aspect-ratio crystalline grain growth for efficient hybrid perovskite solar cells. Nat. Commun. *6*, 7747.
18. Xiao, Z., Dong, Q., Bi, C., Shao, Y., Yuan, Y., and Huang, J. (2014). Solvent annealing of perovskite-induced crystal growth for photovoltaic-device efficiency enhancement. Adv. Mater. *26*, 6503–6509.
19. Zheng, X., Chen, B., Dai, J., Fang, Y., Bai, Y., Lin, Y., Wei, H., Zeng, X.C., and Huang, J. (2017). Defect passivation in hybrid perovskite solar cells using quaternary ammonium halide anions and cations. Nat. Energy *2*, 17102.
20. Shao, Y., Xiao, Z., Bi, C., Yuan, Y., and Huang, J. (2014). Origin and elimination of photocurrent hysteresis by fullerene passivation in $CH_3NH_3PbI_3$ planar heterojunction solar cells. Nat. Commun. *5*, 5784.
21. Tan, H., Jain, A., Voznyy, O., Lan, X., García de Arquer, F.P., Fan, J.Z., Quintero-Bermudez, R., Yuan, M., Zhang, B., Zhao, Y., et al. (2017). Efficient and stable solution-processed planar perovskite solar cells via contact passivation. Science *355*, 722–726.
22. Lee, M.M., Teuscher, J., Miyasaka, T., Murakami, T.N., and Snaith, H.J. (2012). Efficient hybrid solar cells based on meso-superstructured organometal halide perovskites. Science *338*, 643–647.
23. Abate, A., Saliba, M., Hollman, D.J., Stranks, S.D., Wojciechowski, K., Avolio, R., Grancini, G., Petrozza, A., and Snaith, H.J. (2014). Supramolecular halogen bond passivation of organic-inorganic halide perovskite solar cells. Nano Lett. *14*, 3247–3254.
24. Abdi-Jalebi, M., Andaji-Garmaroudi, Z., Cacovich, S., Stavrakas, C., Philippe, B., Richter, J.M., Alsari, M., Booker, E.P., Hutter, E.M., Pearson, A.J., et al. (2018). Maximizing and stabilizing luminescence from halide perovskites with potassium passivation. Nature *555*, 497–501.
25. Rudd, P.N., and Huang, J. (2019). Metal Ions in Halide Perovskite Materials and Devices. Trends Chem. *1*, 394–409.
26. Abdi-Jalebi, M., Pazoki, M., Philippe, B., Dar, M.I., Alsari, M., Sadhanala, A., Divitini, G., Imani, R., Lilliu, S., Kullgren, J., et al. (2018). Dedoping of Lead Halide Perovskites Incorporating Monovalent Cations. ACS Nano *12*, 7301–7311.
27. Zhao, W., Yao, Z., Yu, F., Yang, D., and Liu, S.F. (2017). Alkali Metal Doping for Improved $CH_3NH_3PbI_3$ Perovskite Solar Cells. Adv. Sci. (Weinh.) *5*, 1700131.
28. Saidaminov, M.I., Kim, J., Jain, A., Quintero-Bermudez, R., Tan, H.R., Long, G.K., Tan, F.R., Johnston, A., Zhao, Y.C., Voznyy, O., et al. (2018). Suppression of atomic vacancies via incorporation of isovalent small ions to increase the stability of halide perovskite solar cells in ambient air. Nat. Energy *3*, 648–654.
29. Turren-Cruz, S.H., Saliba, M., Mayer, M.T., Juarez-Santiesteban, H., Mathew, X., Nienhaus, L., Tress, W., Erodici, M.P., Sher, M.J., Bawendi, M.G., et al. (2018). Enhanced charge carrier mobility and lifetime suppress hysteresis and improve efficiency in planar perovskite solar cells. Energy Environ. Sci. *11*, 78–86.
30. Chen, C., Xu, Y., Wu, S., Zhang, S., Yang, Z., Zhang, W., Zhu, H., Xiong, Z., Chen, W., and Chen, W. (2018). CaI_2: a more effective passivator of perovskite films than PbI_2 for high efficiency and long-term stability of perovskite solar cells. J. Mater. Chem. A Mater. Energy Sustain. *6*, 7903–7912.
31. Wang, J.T.W., Wang, Z., Pathak, S., Zhang, W., deQuilettes, D.W., Wisnivesky-Rocca-Rivarola, F., Huang, J., Nayak, P.K., Patel, J.B., Yusof, H.A.M., et al. (2016). Efficient perovskite solar cells by metal ion doping. Energy Environ. Sci. *9*, 2892–2901.
32. Wang, L., Zhou, H., Hu, J., Huang, B., Sun, M., Dong, B., Zheng, G., Huang, Y., Chen, Y., Li, L., et al. (2019). A Eu^{3+}-Eu^{2+} ion redox shuttle imparts operational durability to Pb-I perovskite solar cells. Science *363*, 265–270.
33. Lin, Y., Shao, Y., Dai, J., Li, T., Liu, Y., Dai, X., Xiao, X., Deng, Y., Gruverman, A., Zeng, X.C., and Huang, J. (2021). Metallic surface doping of metal halide perovskites. Nat. Commun. *12*, 7.
34. Bardos, R.A., Trupke, T., Schubert, M.C., and Roth, T. (2006). Trapping artifacts in quasi-steady-state photoluminescence and photoconductance lifetime measurements on silicon wafers. Appl. Phys. Lett. *88*, 053504.
35. Cousins, P.J., Neuhaus, D.H., and Cotter, J.E. (2004). Experimental verification of the effect of depletion-region modulation on photoconductance lifetime measurements. J. Appl. Physiol. *95*, 1854–1858.
36. Lin, Y., Liu, Y., Chen, S., Wang, S., Ni, Z., Van Brackle, C.H., Yang, S., Zhao, J., Yu, Z., and Dai, X. (2021). Revealing defective nanostructured surfaces and their impact on the intrinsic stability of hybrid perovskites. Energy Environ. Sci. *14*, 1563–1572.
37. Edri, E., Kirmayer, S., Henning, A., Mukhopadhyay, S., Gartsman, K., Rosenwaks, Y., Hodes, G., and Cahen, D. (2014). Why lead methylammonium tri-iodide perovskite-based solar cells require a mesoporous electron transporting scaffold (but not necessarily a hole conductor). Nano Lett. *14*, 1000–1004.

38. Wang, Q., Shao, Y., Xie, H., Lyu, L., Liu, X., Gao, Y., and Huang, J. (2014). Qualifying composition dependent p and n self-doping in $CH_3NH_3PbI_3$. Appl. Phys. Lett. *105*, 163508.

39. Saliba, M., Matsui, T., Domanski, K., Seo, J.Y., Ummadisingu, A., Zakeeruddin, S.M., Correa-Baena, J.P., Tress, W.R., Abate, A., Hagfeldt, A., and Grätzel, M. (2016). Incorporation of rubidium cations into perovskite solar cells improves photovoltaic performance. Science *354*, 206–209.

40. Kim, J., Lee, S.H., Lee, J.H., and Hong, K.H. (2014). The Role of Intrinsic Defects in Methylammonium Lead Iodide Perovskite. J. Phys. Chem. Lett. *5*, 1312–1317.

41. Hutter, E.M., Eperon, G.E., Stranks, S.D., and Savenije, T.J. (2015). Charge carriers in planar and meso-structured organic–inorganic perovskites: mobilities, lifetimes, and concentrations of trap states. J. Phys. Chem. Lett. *6*, 3082–3090.

42. Bahrami, B., Chowdhury, A.H., Gurung, A., Mabrouk, S., Reza, K.M., Rahman, S.I., Pathak, R., and Qiao, Q. (2020). Nanoscale spatial mapping of charge carrier dynamics in perovskite solar cells. Nano Today *33*, 100874.

43. Hou, Y., Aydin, E., De Bastiani, M., Xiao, C., Isikgor, F.H., Xue, D.J., Chen, B., Chen, H., Bahrami, B., Chowdhury, A.H., et al. (2020). Efficient tandem solar cells with solution-processed perovskite on textured crystalline silicon. Science *367*, 1135–1140.